COMMUNICATIONS

Magnetic Resonance in Medicine 41:1077–1083 (1999)

Localized In Vivo ^{1}H NMR Detection of Neurotransmitter Labeling in Rat Brain During Infusion of [1-^{13}C] D-Glucose

Josef Pfeuffer, Ivan Tkáč, In-Young Choi, Hellmut Merkle, Kâmil Uğurbil, Michael Garwood, and Rolf Gruetter*

Resolved localized nuclear magnetic resonance (NMR) signals of ^{1}H bound to ^{13}C label in the carbon positions of glutamate C4, C3 and glutamine C4, C3, as well as in aspartate C3, lactate C3, alanine C3, γ-aminobutyric acid C3, and glucose C1 were simultaneously observed in spectra obtained from rat brain in vivo. Time-resolved label incorporation was measured with a new adiabatic carbon editing and decoupling (ACED) single-voxel stimulated echo acquistion mode (STEAM) sequence. Adiabatic carbon broadband decoupling of 12 kHz bandwidth was achieved in vivo, which decoupled the entire ^{13}C spectrum at 9.4 T. Resonances from N-acetyl-aspartate and creatine were also detected, consistent with natural-abundance ^{13}C levels. These results emphasize the potential of ^{1}H NMR for following complex biochemical pathways in *localized* areas of resting rat brain as well as during focal activation using infusions of ^{13}C-labeled glucose. Magn Reson Med 41:1077–1083, 1999.

Key words: localized ^{13}C editing; ACED-STEAM; adiabatic broadband decoupling; neurotransmitter labeling; [1-^{13}C] glucose infusion

In vivo ^{13}C NMR spectroscopy *with localization* is emerging as an important tool for studying intermediary metabolism non-invasively in the brain. The high dispersion of the chemical shift and high spectral resolution make ^{13}C NMR a powerful method for studying neurochemistry (1,2). In brain, ^{13}C NMR has been used for studying Krebs cycle flux and carbon cycling between neurons and glia (3,4). In animals in vivo, the measurement of ^{13}C label has been performed mostly unlocalized, detecting signal from whole brain (4–7), whereas ^{13}C NMR combined with localization is becoming a routine approach in human brain (3,8,9). Localization methods for time-resolved, indirect ^{1}H-detection of ^{13}C label have often been used for observing C4 glutamate, e.g., refs. 10–12, as well as label accumulation in other molecules and positions (13–16).

Proton-detection of ^{13}C label is most often performed in conjunction with three-dimensional localization by inverting the carbon-coupled proton magnetization on alternate scans and using difference editing (11,12,17), or by using heteronuclear single- or multiple-quantum editing techniques (13,14,16,18). In this report, a modification of the stimulated echo acquisition mode (STEAM) localization for the purpose of performing adiabatic carbon editing and decoupling (ACED) is proposed using adiabatic pulses requiring low peak radiofrequency (RF) power.

One major drawback of ^{1}H-detected ^{13}C labeling in vivo has been the difficulty of detecting ^{13}C label in cerebral glutamine. Observation of label incorporation into glutamine is a direct manifestation of glial metabolism and may reflect glutamatergic action due to the known mechanism of glial uptake of neuronal glutamate, e.g., refs. 4, 9, 19, and 20 and references therein. The purpose of this study was to investigate whether the labeling of glutamine and other metabolites can be observed in the ^{1}H spectrum simultaneously with that of glutamate, provided sufficient spectral resolution is present. This objective was achieved using very high magnetic fields combined with higher order shimming methods, i.e. FASTMAP (21). The demonstrated sensitivity is expected to permit direct localized measurements of many neurochemical reactions in resting rat brain as well as during focal activation.

MATERIALS AND METHODS

Three male Sprague-Dawley rats (230–280 g) were anesthetized with 2% isoflurane in 60%/40% O_2/N_2O and ventilated at physiological conditions. Oxygen saturation, maintained above 95%, was continuously monitored with an infrared sensor clipped to the tail (Nonin Medical, Minneapolis, MN). A rectal thermosensor (Cole-Parmer, Vernon Hills, IL) was used to verify that the body temperature was at 310 K, which was maintained by placing the rats on a heated water blanket. A femoral venous line was used for infusion of [1-^{13}C] D-glucose (Isotec, Miamisburg, OH), prepared as 70% enriched, 20% weight/vol solution. In all studies, a bolus of 200 mg glucose was given in the first 5 min, followed by a constant-rate glucose infusion of 16 mg/min, which typically led to modestly elevated plasma glucose concentrations on the order of 16 mM, similar to previous animal studies (15).

The experiments were performed with a Varian INOVA spectrometer (Varian, Palo Alto, CA) interfaced to a 31 cm horizontal bore, 9.4 T magnet (Magnex, Abingdon, UK), which was equipped with an 11 cm actively shielded gradient insert capable of switching 300 mT/m in 500 μsec (Magnex). A quadrature 400 MHz ^{1}H surface RF coil, combined with a linearly polarized, three-turn 100 MHz ^{13}C coil with a diameter of 12 mm, was used for transmit and receive, built according to a previously described design (22). The processing software, written with PV-

Center for Magnetic Resonance Research, Department of Radiology, University of Minnesota Medical School, Minneapolis, Minnesota.

Grant sponsor: NIH; Grant numbers: R01 CA64338 and P41 RR08079; Grant sponsors: the W.M. Keck Foundation and the Whitaker Foundation.

*Correspondence to: Rolf Gruetter, Center for Magnetic Resonance Research, University of Minnesota Medical School, 2021 6th St. SE, Minneapolis, MN 55455. E-mail: gruetter@cmrr.umn.edu

Received 4 August 1998; revised 8 February 1999; accepted 15 March 1999.

WAVE (Visual Numerics, Boulder, CO), allowed automated frequency, phase correction, and peak integration of the metabolite spectra.

To minimize effects of ^{1}H-^{1}H coupling on signal intensity, the localization method was based on a STEAM sequence that is capable of operating at a TE of 1 msec, combined with VAPOR water suppression and interleaved outer volume suppression, as described elsewhere (23). Briefly, asymmetric amplitude-modulated pulses of 500 μsec duration were used for slice selection that generated a 90^0 pulse with a 13.5 kHz bandwidth at a $\gamma B_1/2\pi$ of 3.3 kHz. The seven pulses of the variable pulse power and optimized relaxation delay (VAPOR) water suppression scheme (25 msec duration) did not affect the M_z magnetization by more than 5% outside a region of ±150 Hz (±0.38 ppm) from the water resonance. Outer-volume suppression was performed using six hyperbolic secant pulses of 1.2 msec duration (18.5 kHz bandwidth) for each spatial dimension with different RF power settings.

Shimming of all first- and second-order shim coils was done with FASTMAP (21,24), typically resulting in a 12–14 Hz linewidth of the water resonance in a $7 \times 2.8 \times 7$ mm^3 voxel (137 μl), which was located on the midline 2 mm posterior to bregma and 3 mm ventral. The corresponding linewidth of the metabolite singlet resonances was between 8 and 10 Hz (0.025 ppm).

The localized ACED-STEAM sequence is illustrated in Fig. 1. Coherence pathways generated by the sequence can be analyzed by product-operator formalism, when neglecting homonuclear J_{HH} evolution and chemical shift evolution during the TE/2 period, which was set to the shortest duration that edits the full ^{13}C magnetization, namely, $1/2J_{CH}$ (<4 msec). After the first slice-selective ^{1}H RF pulse and the first TE/2 delay, the ^{13}C (S)-coupled ^{1}H coherences (I) evolve into an $I_{x,y}S_z$ coherence just before the second, slice-selective ^{1}H RF pulse is applied, converting half of the dephased coherence into an I_zS_z state that does not further evolve during TM due to chemical shift or weak J coupling. Coherence selection in the STEAM sequence dictates that the I_yS_z coherences are not refocused, analogous to the I_y coherences (^{1}H) not coupled to ^{13}C. A 15 msec long adiabatic full passage (AFP) pulse of the HS8 type (25) with a 12 kHz bandwidth for 99% inversion efficiency was applied during TM on the carbon channel. Switching this carbon inversion pulse on and off alternately resulted in I_zS_z and $+I_zS_z$, respectively.

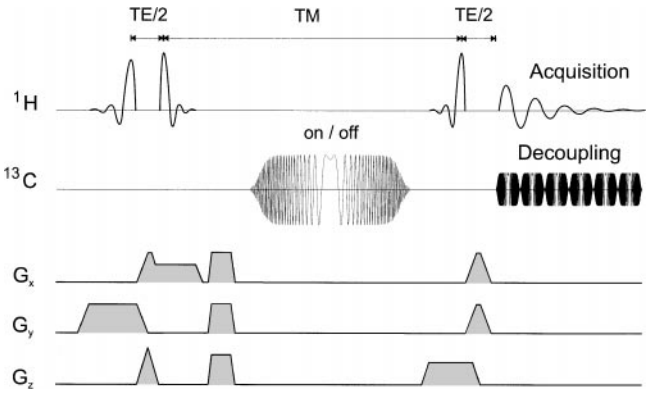

FIG. 1. ACED with single-voxel STEAM localization. TE was set to $1/J_{CH}$, and a 15 msec broadband adiabatic HS8 inversion pulse (25) was applied during TM at δ_{13C} = 35 ppm. Toggling the power of the AFP pulse on and off generated $-I_zS_z$ and $+I_zS_z$ spin states, respectively. Adiabatic ^{13}C broadband decoupling using an HS8 pulse with a five-step phase cycle and MLEV-4 (27) was applied during acquisition, resulting in a 12 kHz decoupling bandwidth.

The third, slice-selective ^{1}H pulse converts the $\pm I_zS_z$ state into, e.g., $\pm I_yS_z$, which is detectable as $\pm I_x$ after the second TE/2 period, resulting in two spectra that are recorded separately, denoted S_{on} and S_{off}, respectively. The relationship $S_{on} = S_{off}$ holds for protons that are not coupled to ^{13}C (I_x), and $S_{on} = -S_{off}$ for the ^{13}C-coupled protons ($-I_x$). Subtraction ($S_{off} - S_{on}$) filters the signal from protons bound to ^{13}C. Inherently, the ^{13}C-decoupled spectrum obtained in the absence of the editing pulse, S_{off}, contains the total ^{1}H signals bound to ^{12}C *and* ^{13}C. The theoretical signal dependence with respect to J_{CH} was determined from the product-operator analysis (not shown) to be proportional to $\cos(\pi TE/J_{CH})$. Optimal sensitivity for the editing process with respect to TE is therefore achieved when $TE = 1/J_{CH}$. We used the TE appropriate for $J_{CH} \sim 127$ Hz of aspartate (Asp), creatine (Cr), glutamine (Gln), glutamate (Glu), lactate (Lac), and N-acetyl-aspartate (NAA) or for $J_{CH} \sim 167$ Hz of glucose (Glc), respectively. Using a 32-step phase cycling scheme and a TR of 4 sec resulted in a temporal resolution of approximately 5 min. From line-broadened phantom spectra acquired with the same experimental conditions as in vivo, homonuclear coupling due to J_{HH} reduced the intensity of the strongly coupled spins systems of glutamate and glutamine by at most 5% (not shown). At longer echo times, such as a TE of 20 msec, substantial reduction in signal intensity has been reported (23).

Adiabatic decoupling in the carbon channel was applied during the entire acquisition time of 400 msec. Two different AFP pulses were used: a 1.8 msec long tanh/tan pulse with R = 54 (26) and a 1.5 msec long HS8 with R = 20 (25). In both decoupling patterns, a five-step phase cycle combined with MLEV-4 was used, as described previously (27). With the tanh/tan shape, a ^{13}C decoupling bandwidth of 4 kHz (corresponding to 40 ppm at 9.4 T) was achieved. With the HS8 pulse, the decoupling bandwidth was 12 kHz (corresponding to 120 ppm). The peak decoupler $\gamma B_2/2\pi$ was approximately 1 kHz, and peak decoupling power was below 2 W. No heating effects were observed in phantoms.

Phantom studies were performed on 5 M natural-abundance acetate and [1-^{13}C] D-glucose. The performance of the ^{13}C-editing/inversion pulse applied during TM was verified to produce a 99% inversion of ^{13}C satellites over more than 12 kHz, resulting in a 120 ppm editing bandwidth (not shown).

RESULTS

A carbon-edited spectrum of the rat brain in vivo obtained during 200 min of ^{13}C-labeled glucose infusion is shown in Fig. 2a. Adiabatic carbon decoupling using the tanh/tan pulse was applied at 35 ppm in the ^{13}C channel (δ_{13C} = 35ppm). In the ^{13}C-edited ^{1}H spectrum, only protons bound to ^{13}C in different metabolites were thus observed. The two interleaved recorded spectra, S_{on} and S_{off}, were subtracted

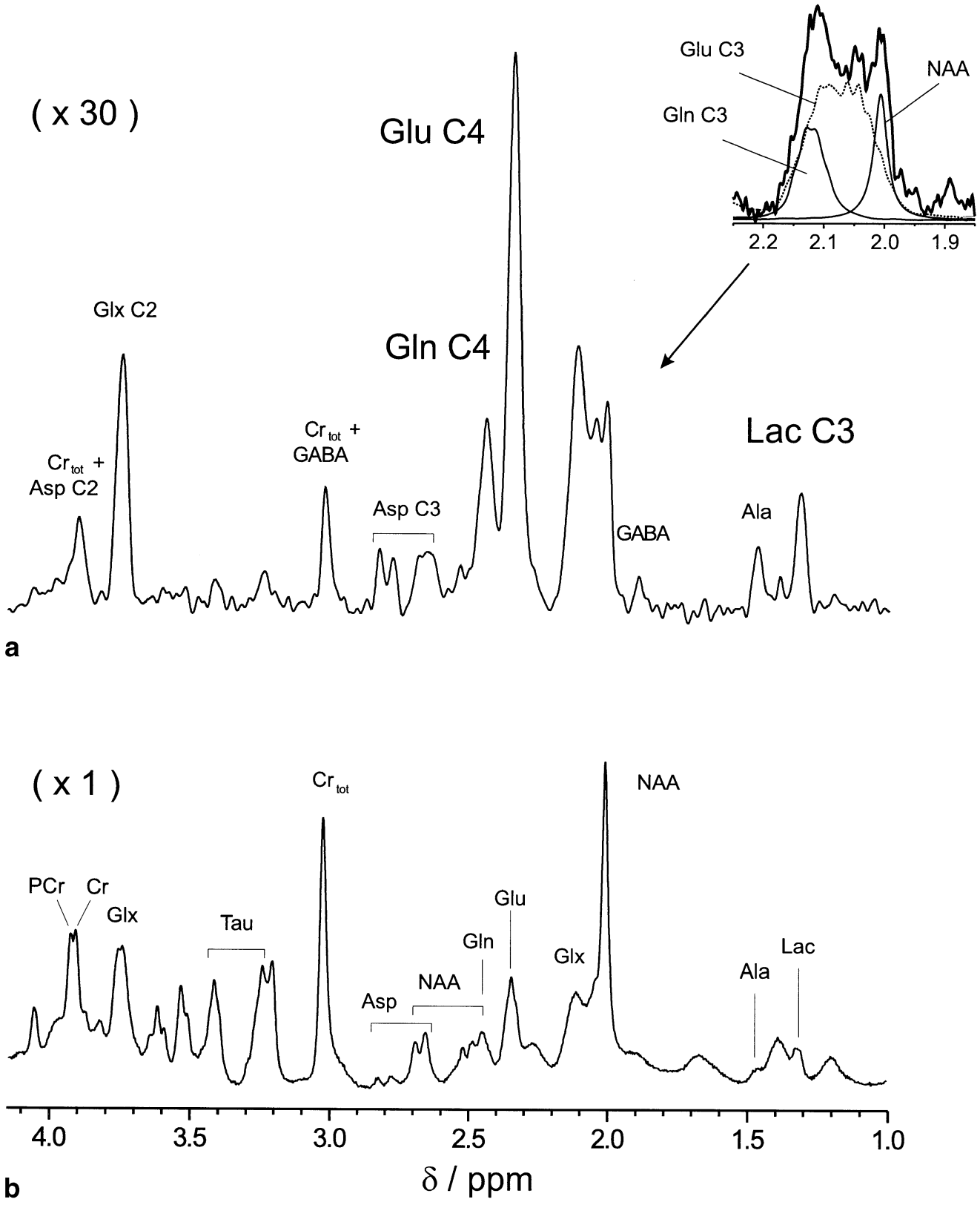

FIG. 2. ^{13}C-edited and broadband-decoupled ACED-STEAM spectrum obtained with the sequence in Fig. 1 from a 137 µl volume in rat brain in vivo during infusion of [1-^{13}C] glucose (TE 7.9 msec, TM 20 msec, TR 4 sec). **a:** ^{13}C-edited ^{1}H spectrum obtained by subtracting spectra acquired with the inversion pulse of ACED-STEAM on and off, respectively (S_{off} - S_{on}, 2560 transients). Only signals from protons bound to ^{13}C are detected. Peak assignments were based on resonance position, line width, and relative intensity, being consistent with total concentration and fractional enrichment of glutamate. The inset illustrates the ability to distinguish ^{13}C label between glutamate C3 and glutamine C3 by comparing the in vivo spectrum (solid line) to line-broadened solution spectra of Glu, Gln, and NAA (thin lines). The spectrum was processed with 5.3 Hz Gaussian linebroadening. **b:** The reference ^{1}H spectrum gained from the same data set as in a, averaging only the scans when the editing pulse was off (S_{off}, 1280 transients). No apodization was applied (fast Fourier transform only). The normalized vertical scale in a is 30-fold expanded compared with b. No baseline correction was applied.

and yielded the ^{1}H-^{13}C resonances, edited for J_{CH} = 127 Hz (Fig. 2a, 2560 excitations). The non-edited ^{1}H spectrum (S_{off}) in Fig. 2b (1280 excitations) is equivalent to a standard ^{1}H spectrum acquired in the absence of ^{13}C label in the infusate. For comparison, the vertical scale was normalized by the number of transients and increased by a factor of 30 in Fig. 2a. The peak labels of the ^{1}H-detected carbon positions were abbreviated, e.g., Glu C4 represents all glutamate isotopomers containing a ^{13}C at position C4. Chemical shifts were referenced to NAA at 2.009 ppm.

In addition to the dominant proton C4 resonance of glutamate (Glu) at 2.34 ppm, a resolved peak from the C4 of glutamine (Gln) was observed at 2.44 ppm in the spectrum shown in Fig. 2a, which was obtained after subtracting S_{on} from S_{off}. Other ^{13}C-edited ^{1}H resonances from less concentrated metabolites were observed for protons coupled to the C3 of lactate (Lac) at 1.32 ppm and C3 of alanine (Ala) at 1.47 ppm. The relative intensities of Ala and Lac observed in the edited spectrum (Fig. 2b) are approximately proportional to the relative signals in S_{off} (Fig. 2a). Protons coupled to the C3 of aspartate (Asp) at 2.80 and 2.65 ppm were also clearly detected, whereas the linewidth of the peak at 3.90 ppm in Fig. 2b was much narrower than expected for aspartate from line-broadened solution spectra (not shown), suggesting signal contributions from natural-abundance creatine and phosphocreatine (Cr_{tot} = Cr + PCr). Likewise, the linewidth of the peak at 3.02 ppm (Fig. 2b) was much narrower than expected for the C4 of γ-aminobutyric acid (GABA), and the intensity was consistent with a significant contribution from natural-abundance creatine plus phosphocreatine at 3.02 ppm. GABA C3, however, was observed as a resolved peak at 1.89 ppm in the ^{13}C–edited spectrum. An upfield shoulder was observed at the C4 glutamate resonance consistent with label being incorporated into the C2 of GABA at 2.30 ppm. Two peaks were observed at 3.41 and at 3.24 ppm, tentatively consistent with natural-abundance taurine (Tau) resonances.

Furthermore, the inset in Fig. 2a shows the spectral region corresponding to the C3 resonances of glutamate and glutamine. The measured spectral pattern (solid line) was inconsistent with either glutamate, glutamine or NAA alone, but could be explained as a superposition of all three resonances. The different spectral pattern of C3 glutamine and C3 glutamate implies that these resonances can be separated in our setting using peak deconvolution methods.

To verify the ^{13}C broadband decoupling performance in vivo, edited spectra were recorded interleaved with and without HS8 decoupling applied at δ_{13C} = 35 ppm. As shown in Fig. 3a, the [1-^{13}C] α-D-glucose (δ_{1H} = 5.23 ppm, δ_{13C} = 93 ppm) and the lactate methyl (δ_{1H} = 1.32 ppm, δ_{13C} = 21 ppm) were simultaneously decoupled. The peak area of the decoupled glucose peak was at least 70% of that of the corresponding doublet peaks (dashed lines) in the coupled spectrum (Fig. 3b), reflecting some signal loss into cycling sidebands. Considering that the [1-^{13}C] glucose resonance is near the edge of the decoupling bandwidth since the decoupling frequency was applied at 35 ppm, this performance is still impressive and implies a decoupling bandwidth in vivo of approximately 12 kHz. Note the detection of the coupled lactate doublet despite a low cerebral lactate concentration in resting normal rat brain (Fig. 2b).

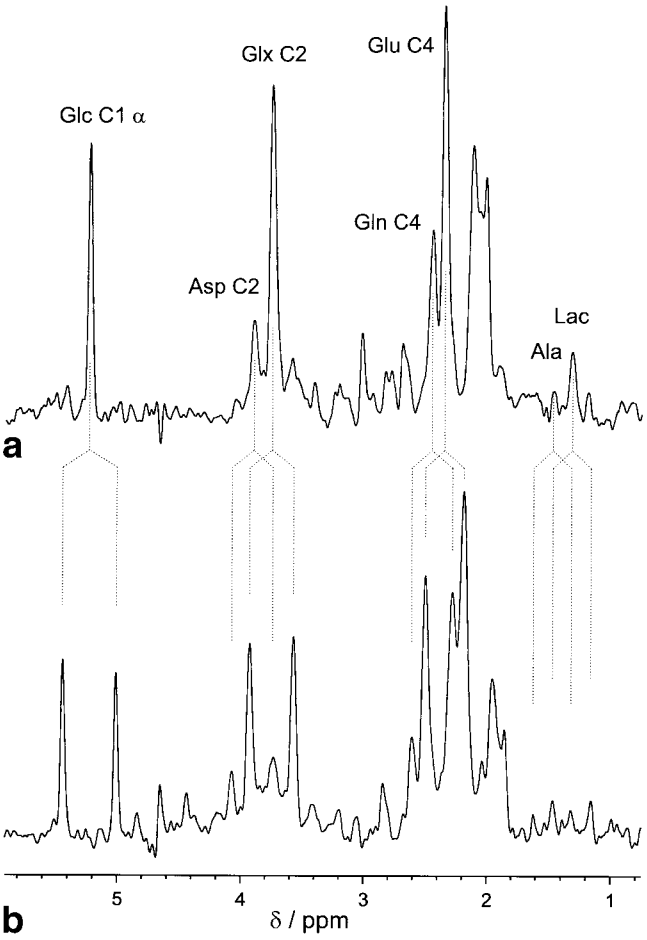

FIG. 3. Adiabatic carbon-edited ^{1}H NMR spectrum (ACED-STEAM) in rat brain demonstrating the feasibility of adiabatic broadband decoupling in vivo, (**a**) acquired with the HS8 decoupling scheme and (**b**) acquired without decoupling. (TE 6 msec, TM 20 msec, TR 4 sec). The ^{13}C decoupler frequency was at δ_{13C} = 35 ppm. Note that J_{CH} for glucose C1 is distinctly larger than that for most other peaks. The dotted lines indicate the J_{CH} couplings. To minimize effects due to small frequency drifts, a and b were acquired in an interleaved fashion at t = 190–220 min from the same animal used for Fig. 4. Spectra were processed with 6.4 Hz Gaussian linebroadening. No baseline correction was applied.

To demonstrate the ability of ACED-STEAM to measure time-resolved incorporation of label into different pools, spectra summed over 15 min are shown in Fig. 4 (192 excitations). The turnover of ^{13}C label in rat brain in vivo was followed during infusion of [1-^{13}C] glucose. Note that label accumulation in metabolites with low concentration such as lactate was observable.

The ^{13}C label incorporation into the C4 of glutamate and glutamine was assessed by integration of the corresponding peaks in the edited ^{1}H spectra averaged over 5 min (Fig. 5a, 64 excitations). Spectra averaged over 15 min (Fig. 5b, 192 excitations) were integrated for the other peaks such as glucose, lactate, aspartate, and GABA. The signal intensities in Fig. 5 were derived from S_{off} - S_{on} estimated at t >120 min relative to the total creatine methyl resonance Cr_{tot} at 3.0 ppm integrated in S_{off}, assuming a concentration of

FIG. 4. Carbon ^{13}C turnover in rat brain in vivo during infusion of [1-^{13}C] glucose as detected by ACED-STEAM (TE 7.9 msec, TM 20 msec, TR 4 sec). The transients were averaged over 15 min (192 excitations) and are shown after 4.5 Hz Gaussian linebroadening. No baseline correction was applied. The data are from the same animal used for Fig. 2.

8.5μmol/g and taking into account the number of protons contributing to the respective resonances. ^{1}H detection of ^{13}C label of C4 of glutamate and glutamine yielded a root-mean-square deviation estimated at 0.08 μmol/g (averaged over 5 min) from the residuals of a linear regression performed at t >120 min in Fig. 5. Likewise, for lactate, aspartate, and GABA the root-mean-square deviation was estimated to be on the order of 0.1 μmol/g wet weight (averaged over 15 min).

DISCUSSION

The potentially higher sensitivity of ^{1}H NMR for detecting ^{13}C label has been previously exploited for the ^{1}H-detection of label in glutamate C4 (11,12,28,29), in elevated lactate in tumors (18,29,30), and in [1-^{13}C] glucose during hyperglycemia (15). The present study demonstrates the ability of ^{1}H NMR to detect label in many additional metabolites, such as glutamine, aspartate, GABA, and alanine. In addition, detection of label incorporation into resting lactate, GABA, and alanine in normal rat brain is reported for the first time. Although adiabatic decoupling was first applied in vivo for ^{1}H-decoupled ^{31}P MRS (31), this study demonstrates the ability of adiabatic pulses to decouple efficiently almost the entire ^{13}C chemical shift range in vivo. Time-resolved lactate labeling was readily detected in 15 min *localized* spectra (Fig. 3), despite a low resting lactate concentration. The scatter due to noise was estimated to be on the order of 0.1μmol/g, suggesting adequate sensitivity for measuring metabolic fluxes.

A STEAM sequence designed for echo times of 1 msec (23) was used for localization, which allowed the shortest possible editing time and thus minimized homonuclear

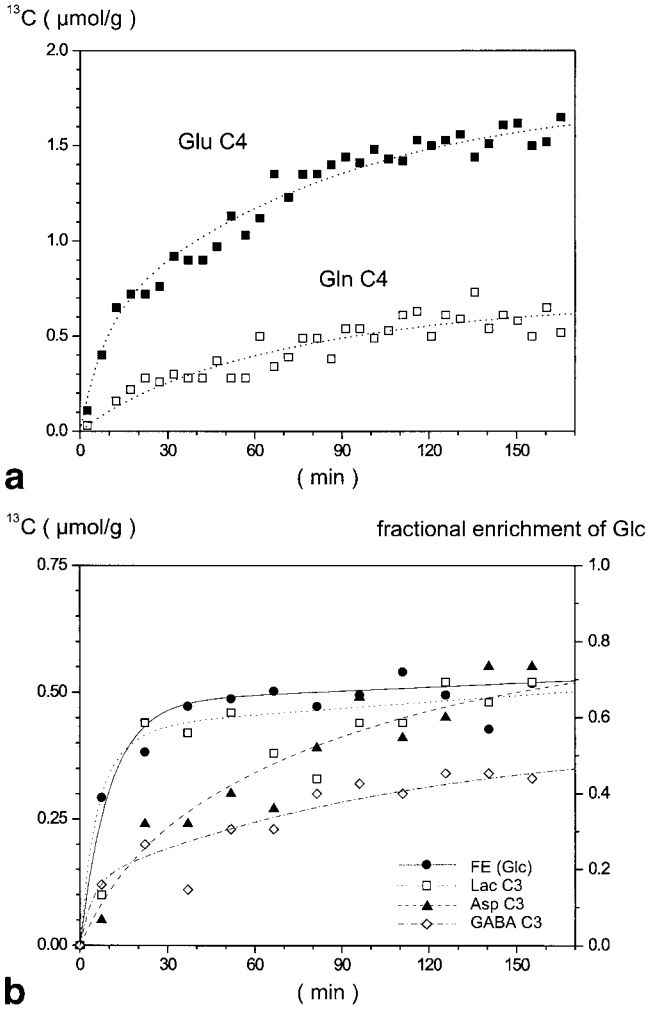

FIG. 5. Temporal evolution of ^{13}C-labeled metabolite concentrations during infusion of [1-^{13}C] glucose acquired from a different animal. **a:** The time course of ^{13}C incorporation into glutamate C4 (■) and glutamine C4 (□) is shown over a 165 min period during which a constant-rate infusion of 70% enriched glucose was applied. **b:** The label incorporation into low-concentration metabolites (left scale) for the lactate C3 (□), aspartate C3 (▲), and γ-aminobutyric acid C3 (◇) is shown. The fractional enrichment of brain glucose (●, right scale) was calculated from the ^{13}C glucose satellite intensity compared with the total glucose signal at the H1 α position. Multi-exponential curves were fitted for better visualization.

proton-proton J_{HH} evolution and T_2 loss ($TE = 1/J_{CH} < 8$ msec). Highly efficient VAPOR water suppression (23) and outer-volume suppression led to a high signal stability, which made the incorporation of an add-subtract scheme feasible for ^{13}C editing. This was achieved by applying an adiabatic full-passage pulse of the HS8 type (25) in the TM period, which is a rather simple modification of the STEAM sequence. The long sweep duration of 15 msec over 12 kHz resulted in low peak B_1 demands for inversion. Simulations of this pulse shape showed that 99% of the magnetization is inverted at $\gamma B_1/2\pi$ above 0.7 kHz, thus allowing much of the sensitive volume of the small ^{13}C coil to be fully inverted.

Broadband decoupling was achieved by turning on pattern decoupling during acquisition using phase-cycled adiabatic HS8 pulses. The advantages of such an adiabatic decoupling scheme were the much-increased bandwidth of 12 kHz covered at a low peak B_2 when using HS8 pulses and the B_1 insensitivity of the scheme used. Overall, the two simple modifications to the STEAM sequence were made with minimal pulse programming effort.

The sensitivity achieved from 137 μl volumes (Fig. 5) suggested that the determination of metabolic fluxes using complex two-compartment models of cerebral metabolism is feasible in animal brain, similar to those recently proposed for human brain (9). This modified STEAM sequence may be an alternative to some of the more complicated editing sequences when spatial resolution is not critical and pulse programming capabilities are limited.

Compared with some localization methods, the signal of STEAM is reduced by 50%. To make up for the loss in sensitivity, each of the three dimensions of a cubic volume can be increased by 26%, which in many cases may still provide sufficient spatial resolution. The reduction in sensitivity or spatial resolution, however, may be more than offset by the ease of achieving broadband editing. Furthermore, a well-defined voxel definition is easily achievable with STEAM, which has reduced demands on peak RF power, allows minimal signal contamination from the outer volume, and provides a wealth of metabolic information. Whether other, potentially more sensitive techniques can recover the full sensitivity improvements for the given B_1 inhomogeneity and bandwidth with the same advantages of short TE remains to be shown. An important experimental factor for the high spectral quality was certainly the higher-order shimming based on FASTMAP (21,24). Further sensitivity improvements are possible when the fractional enrichment of pyruvate is doubled by using [1,6-$^{13}C_2$] instead of [1-^{13}C] glucose for infusion and are expected to lead to an improved measurement of GABA and lactate labeling.

The demonstrated information gain for ^1H NMR detection of ^{13}C labeling with an add-subtract editing scheme can be naturally combined with the measurement of many metabolites in the ^1H spectrum, S_{off}, (Fig. 2b). It has been well established that metabolite concentrations do not change during hyperglycemia much higher than what was achieved here, in agreement with the low K_m of hexokinase (see ref. 32 and references therein). The resolution achieved at 9.4 T allowed the detection of total tissue glucose, lactate as well as the partially resolved peak from the CH_2 resonance of PCr (21,23). Thus, a comprehensive evaluation of cerebral energy metabolism using ^{13}C infusions with simultaneous measurement of lactate, glucose, and phosphocreatine content is now feasible. Previous studies reported measurements of lactate and glucose content without concomitant ^{13}C turnover data. The results also show that ^{13}C label in glutamate C3 and glutamine C3 can be distinguished in ^1H NMR spectra.

CONCLUSIONS

The localized, simultaneous ^1H NMR detection of glutamate and glutamine ^{13}C labeling at the C4 as well as at the C3 position is feasible; such detection is also feasible in lactate, aspartate, GABA, and glucose. The spectral resolution achieved in the subspectra of the editing process suggests that the tissue levels of phosphocreatine, lactate, and glucose can be monitored simultaneously. These capabilities further suggest that the number of metabolic reactions that can be assessed in localized areas of the rat brain can be substantially increased over what has been achieved previously from measuring glutamate and glutamine C4 alone. Such measurements have the potential to further the understanding of the relationship of brain energy metabolism and neurotransmission during focal activation in normal and diseased brain. Considering the ongoing installation of ultra-high-field human MR systems (7–8 T), extensions to the human brain with similar information content are conceivable.

REFERENCES

1. Bachelard H, Badar-Goffer R. NMR spectroscopy in neurochemistry. J Neurochem 1993;61:412–429.
2. van Zijl PCM, Rothman D. NMR studies of brain C-13-glucose uptake and metabolism—present status. Magn Reson Imaging 1995;13:1213–1221.
3. Gruetter R, Novotny EJ, Boulware SD, Mason GF, Rothman DL, Prichard JW, Shulman RG. Localized ^{13}C NMR spectroscopy of amino acid labeling from [1-^{13}C] D-glucose in the human brain. J Neurochem 1994;63:1377–1385.
4. Sibson NR, Dhankhar A, Mason GF, Behar KL, Rothman DL, Shulman RG. In vivo ^{13}C NMR measurements of cerebral glutamine synthesis as evidence for glutamate-glutamine cycling. Proc Natl Acad Sci USA 1997;94:2699–2704.
5. Cerdan S, Kunnecke B, Seelig J. Cerebral metabolism of [1,2-$^{13}C2$]acetate as detected by in vivo and in vitro ^{13}C NMR. J Biol Chem 1990;265:12916–12926.
6. Kunnecke B, Cerdan S, Seelig J. Cerebral metabolism of [1,2-$^{13}C2$]glucose and [U-$^{13}C4$]3-hydroxybutyrate in rat brain as detected by ^{13}C NMR spectroscopy. NMR Biomed 1993;6:264–277.
7. Artemov D, Bhujwalla ZM, Glickson JD. In vivo selective measurement of (1-^{13}C)-glucose metabolism in tumors by heteronuclear cross polarization. Magn Reson Med 1995;33:151–155.
8. Gruetter R, Novotny EJ, Boulware SD, Rothman DL, Mason GF, Shulman GI, Shulman RG, Tamborlane WV. Direct measurement of brain glucose concentrations in humans by ^{13}C NMR spectorscopy. Proc Natl Acad Sci USA 1992;89:1109–1112.
9. Gruetter R, Seaquist E, Kim S-W, Ugurbil K. Localized in vivo ^{13}C NMR of glutamate metabolism. Intitial results at 4 Tesla. Dev Neurosci 1998;20:380–388.
10. Lukkarinen J, Oja JM, Turunen M, Kauppinen RA. Quantitative determination of glutamate turnover by ^1H-observed, ^{13}C-edited nuclear magnetic resonance spectroscopy in the cerebral cortex ex vivo: interrelationships with oxygen consumption. Neurochem Int 1997;31:95–104.
11. Hyder F, Rothman DL, Mason GF, Rangarajan A, Behar KL, Shulman

RG. Oxidative glucose metabolism in rat brain during single forepaw stimulation: a spatially localized ^{1}H[^{13}C] nuclear magnetic resonance study. J Cereb Blood Flow Metab 1997;17:1040–1047.
12. Fitzpatrick SM, Hetherington HP, Behar KL, Shulman RG. The flux from glucose to glutamate in the rat brain in vivo as determined by ^{1}H-observed, ^{13}C-edited NMR spectroscopy. J Cereb Blood Flow Metab 1990;10:170–179.
13. Inubushi T, Morikawa S, Kito K, Arai T. ^{1}H-detected in vivo ^{13}C NMR spectroscopy and imaging at 2T magnetic field: efficient monitoring of ^{13}C-labeled metabolites in the rat brain derived from 1-^{13}C-glucose. Biochem Biophys Res Commun 1993;191:866–872.
14. van Zijl PCM, Chesnick AS, DesPres D, Moonen CTW, Ruiz-Cabello J, Van Gelderen P. In vivo proton spectroscopy and spectroscopic imaging of [1-^{13}C]-glucose and its metabolic products. Magn Reson Med 1993;30: 544–551.
15. Van Zijl PC, Davis D, Eleff SM, Moonen CT, Parker RJ, Strong JM. Determination of cerebral glucose transport and metabolic kinetics by dynamic MR spectroscopy. Am J Physiol 1997;273:E1216–E1227.
16. Watanabe H, Umeda M, Ishihara Y, Okamoto K, Oda M, Oshio K, Kanamatsu T, Tsukada Y. Multivoxel ^{1}H-^{13}C HSQC spectroscopy using multislice techniques with a 2IzSz state. In: Proceedings of the ISMRM 5th Annual Meeting, Vancouver, BC, 1997. p 1436.
17. Pan JLW, Mason GF, Vaughan JT, Chu WJ, Zhang YT, Hetherington HP. C-13 editing of glutamate in human brain using J-refocused coherence transfer spectroscopy at 4.1 T. Magn Reson Med 1997;37:355–358.
18. deGraaf R, Luo Y, Terpstra M, Garwood M. Spectral editing with adiabatic pulses. J Magn Reson B 1995;109:184–193.
19. Kanamori K, Ross BD, Kuo EL. Dependence of in vivo glutamine synthetase activity on ammonia concentration in rat brain studied by ^{1}H - ^{15}N heteronuclear multiple-quantum coherence-transfer NMR. Biochem J 1995;311:681–688.
20. Magistretti P, Pellerin L. Cellular mechanisms of brain energy metabolism. Relevance to functional brain imaging and to neurodegenerative disorders. Ann NY Acad Sci 1996;777:380–387.
21. Gruetter R, Weisdorf SA, Rajanayagan V, Terpstra M, Merkle H, Truwit CL, Garwood M, Nyberg SL, Ugurbil K. Resolution Improvements in in vivo ^{1}H NMR spectra with increased magnetic field strength. J Magn Reson 1998;135:260–264.
22. Adriany G, Gruetter R. A half volume coil for efficient proton decoupling in humans at 4 Tesla. J Magn Reson 1997;125:178–184.
23. Tkac I, Starcuk Z, Choi I-Y, Gruetter R. In vivo ^{1}H NMR spectroscopy of rat brain at 1 msec echo time. Magn Reson Med 1999;41:649–656.
24. Gruetter R. Automatic, localized in vivo adjustment of all first- and second-order shim coils. Magn Reson Med 1993;29:804–811.
25. Tannus A, Garwood M. Improved performance of frequency-swept pulses using offset-independent adiabaticity. J Magn Reson A 1996;120: 133–137.
26. Hwang TL, van Zijl PCM, Garwood M. Fast broadband inversion by adiabatic pulses. J Magn Reson 1998;133:200–203.
27. Fujiwara T, Anai T, Kurihara N, Nagayama K. Frequency-switched composite pulses for decoupling carbon-13 spins over ultrabroad bandwidths. J Magn Reson A 1993;104:103–105.
28. Rothman DL, Novotny EJ, Shulman GI, Howseman AM, Petroff OA, Mason G, Nixon T, Hanstock CC, Prichard JW, Shulman RG. ^{1}H-[^{13}C] NMR measurements of [4-^{13}C]glutamate turnover in human brain. Proc Natl Acad Sci USA 1992;89:9603–9606.
29. Terpstra M, Gruetter R, High WB, Mescher M, DelaBarre L, Merkle H, Garwood M. Lactate turnover in rat glioma measured by in vivo nuclear magnetic resonance spectroscopy. Cancer Res 1998;58:5083–5088.
30. Schupp DG, Merkle H, Ellermann JM, Ke Y, Garwood M. Localized detection of glioma glycolysis using edited ^{1}H MRS. Magn Reson Med 1993;30:18–27.
31. Luyten PR, Bruntink G, Sloff FM, Vermeulen JW, van der Heijden J, den Hollander JA, Heerschap A. Broadband proton decoupling in human ^{31}P NMR spectroscopy. NMR Biomed 1989;1:177–183.
32. Gruetter R, Ugurbil K, Seaquist ER. Steady-state cerebral glucose concentrations and transport in the human brain. J Neurochem 1998;70: 397–408.